Hindawi Publishing Corporation
ISRN Tribology
Volume 2013, Article ID 482604, 6 pages
http://dx.doi.org/10.5402/2013/482604

Research Article

Performance of Magnetic-Fluid-Based Squeeze Film between Longitudinally Rough Elliptical Plates

P. I. Andharia[1] and G. M. Deheri[2]

[1] *Department of Mathematics, M. K. Bhavnagar University, Bhavnagar, Gujarat 364002, India*
[2] *Department of Mathematics, S. P. University, Vallabh Vidyanagar, Gujarat 388120, India*

Correspondence should be addressed to P. I. Andharia; pareshandharia@yahoo.com

Received 20 November 2012; Accepted 17 December 2012

Academic Editors: J. De Vicente, N. Gerolymos, and J. H. Jang

An attempt has been made to analyze the performance of a magnetic fluid-based-squeeze film between longitudinally rough elliptical plates. A magnetic fluid is used as a lubricant while axially symmetric flow of the magnetic fluid between the elliptical plates is taken into consideration under an oblique magnetic field. Bearing surfaces are assumed to be longitudinally rough. The roughness of the bearing surface is characterized by stochastic random variable with nonzero mean, variance, and skewness. The associated averaged Reynolds' equation is solved with appropriate boundary conditions in dimensionless form to obtain the pressure distribution leading to the calculation of the load-carrying capacity. The results are presented graphically. It is clearly seen that the magnetic fluid lubricant improves the performance of the bearing system. It is interesting to note that the increased load carrying capacity due to magnetic fluid lubricant gets considerably increased due to the combined effect of standard deviation and negatively skewed roughness. This performance is further enhanced especially when negative variance is involved. This paper makes it clear that the aspect ratio plays a prominent role in improving the performance of the bearing system. Besides, the bearing can support a load even when there is no flow.

1. Introduction

The transient load carrying capacity of a fluid film between two surfaces having a relative normal velocity plays a crucial role in frictional devices such as clutch plates in automatic transmissions. Archibald [1] studied the behaviour of squeeze film between various geometrical configurations. Subsequently, Wu [2, 3] investigated the squeeze film performance mainly for two types of geometries, namely, annular and rectangular when one of the surfaces was porous faced. Prakash and Vij [4] discussed the load carrying capacity and time height relations for squeeze film performance between porous plates. In that study various geometries such as circular, annular, elliptical, rectangular, conical, and truncated conical were considered. Besides, a comparison was made between the squeeze film performance of various geometries of equivalent surface area and it was established that the circular geometry registered the highest transient load carrying capacity, other parameters remaining same.

The above studies dealt with conventional lubricant. Verma [5] considered the application of magnetic fluid as a lubricant. The magnetic fluid consisted of fine magnetic grains coated with a surfactant and dispersed in a nonconducting magnetically passive solvent. Later on, Bhat and Deheri [6] discussed the squeeze film behaviour between porous annular disks using a magnetic fluid lubricant with the external magnetic field, oblique to the lower disk. This analysis was improved further by Bhat and Deheri [7] to deal with the performance of a magnetic fluid based squeeze film in curved circular plates. Furthermore, Patel and Deheri [8] studied the behaviour of a magnetic fluid based squeeze film between porous conical plates. All these above studies established that the performance of the bearing system was modified and enhanced owing to the magnetic fluid lubricant.

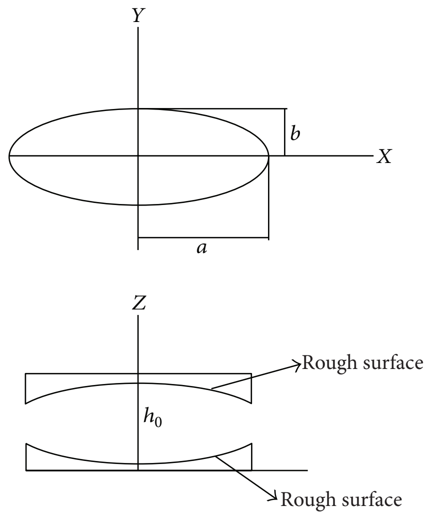

FIGURE 1: Bearing configuration.

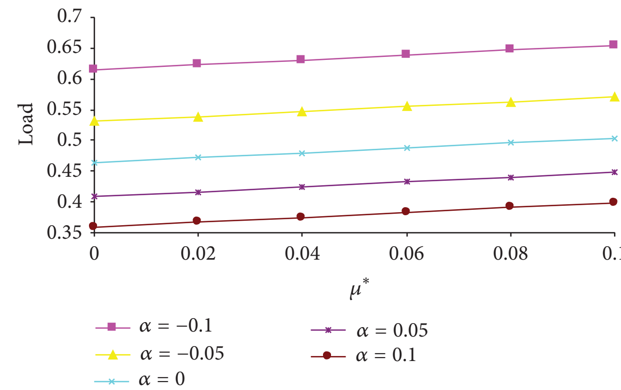

FIGURE 2: Variation of load carrying capacity with respect to μ^* for different α.

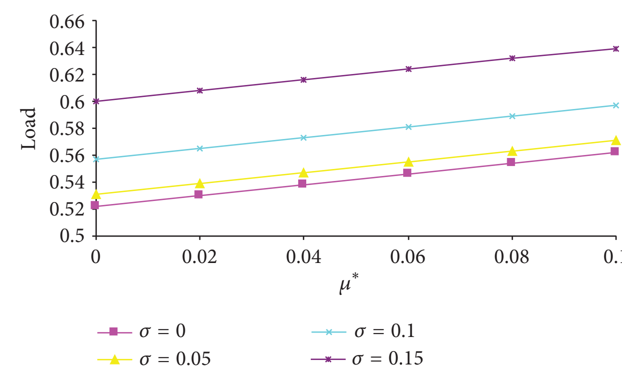

FIGURE 3: Variation of load carrying capacity with respect to μ^* for different σ.

In all the above analyses bearing surfaces were assumed to be smooth. However, the bearing surfaces after having some run-in and wear develop roughness. In fact, due to elastic, thermal, and uneven wear effects, the configurations encountered in practice are usually far from smooth. Sometimes the contamination of the lubricant and chemical degradation of the surfaces result in roughness. The roughness appears to be random in character, which was recognized by many investigators who analyzed the effect of surface roughness resorting to a stochastic method [9–13]. Christensen and Tonder [14–16] mathematically modelled the random roughness and suggested a comprehensive general analysis for investigating the effect of transverse as well as longitudinal surface roughness. This approach of Christensen and Tonder was the basis for investigating the effect of surface roughness in a number of investigations [17–24].

Recently, Andharia and Deheri [25] discussed the performance of a magnetic fluid based squeeze film in longitudinally rough conical plates. Here it has been proposed to study and analyze the performance of a squeeze film between longitudinally rough elliptical plates under the presence of a magnetic fluid lubricant.

2. Analysis

The configuration of the bearing system shown in Figure 1 consists of two elliptical plates. The upper plate moves normally towards the lower plate with uniform velocity $\dot{h}_0(= dh_0/dt)$ where h_0 is the central film thickness. The assumptions of usual hydrodynamic lubrication theory are taken into consideration in the analysis. The lubricant film is considered to be isoviscous and incompressible and the flow is laminar.

The bearing surfaces are assumed to be longitudinally rough. The thickness h of the lubricant film is

$$h = \overline{h} + h_s, \tag{1}$$

where $\overline{h}$ is the mean film thickness and h_s is the deviation from the mean film thickness characterizing the random roughness of the bearing surfaces. h_s is considered to be stochastic in nature and governed by the probability density function $f(h_s)$, $-c \le h_s \le c$, where c is the maximum deviation from the mean film thickness. The mean α, the standard deviation σ and the parameter ε which is the measure of symmetry, of the random variable h_s, are defined by the relationships:

$$\alpha = E(h_s), \qquad \sigma^2 = E\left[(h_s-\alpha)^2\right], \tag{2}$$

$$\varepsilon = E\left[(h_s-\alpha)^3\right], \tag{3}$$

where E denotes the expected value defined by

$$E(R) = \int_{-c}^{c} R f(h_s)\, dh_s, \tag{4}$$

wherein

$$f(h_s) = \begin{cases} \dfrac{35}{32}\left(1-\dfrac{h_s^2}{c^2}\right)^3, & -c \le h_s \le c \\ 0, & \text{otherwise.} \end{cases} \tag{5}$$

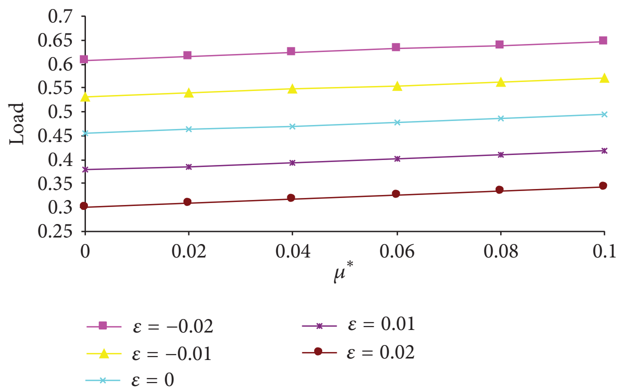

FIGURE 4: Variation of load carrying capacity with respect to μ^* for different ε.

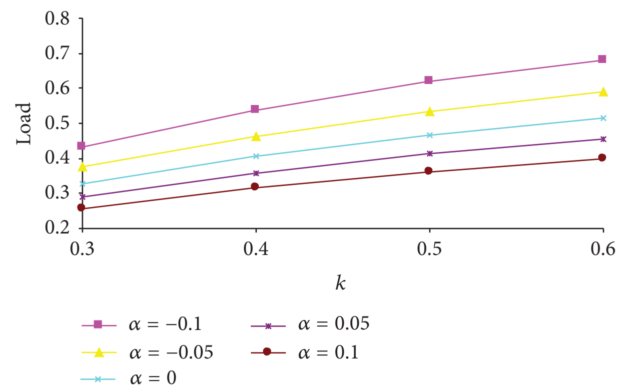

FIGURE 6: Variation of load carrying capacity with respect to k for different α.

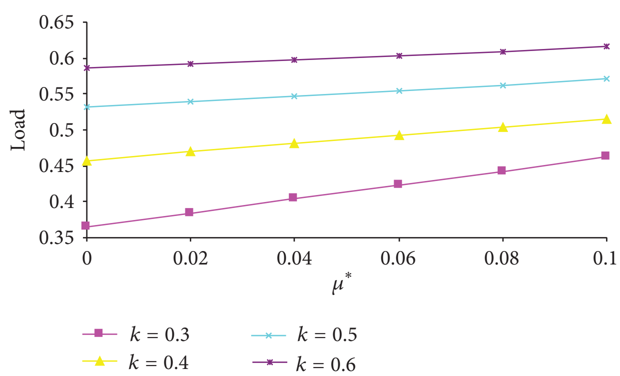

FIGURE 5: Variation of load carrying capacity with respect to μ^* for different k.

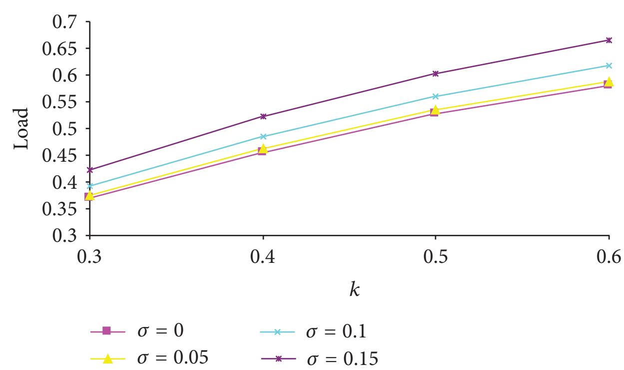

FIGURE 7: Variation of load carrying capacity with respect to k for different σ.

Axially symmetric flow of magnetic fluid between the elliptical plates is taken into consideration under an oblique magnetic field $\overline{M}$ whose magnitude M is expressed as

$$M^2 = ab\left(1 - \frac{x^2}{a^2} - \frac{z^2}{b^2}\right), \tag{6}$$

where a is semimajor axis and b is semiminor axis. The direction of the magnetic field is significant since $\overline{M}$ needs to satisfy the equations

$$\nabla \cdot \overline{M} = 0, \qquad \nabla \times \overline{M} = 0. \tag{7}$$

Therefore, $\overline{M}$ arises out of a potential function and the inclination θ of the magnetic field $\overline{M}$ with the lower plate is determined from

$$\cot\theta \frac{\partial\theta}{\partial x} + \frac{\partial\theta}{\partial z} = \frac{bx + az - xz + 1}{(ab - ax + bz)\, xz + abx^2z^2}. \tag{8}$$

Following Prakash and Vij [4], Bhat and Deheri [6], and Andharia and Deheri [25], the Reynolds' equation governing the film pressure p in the present case is obtained as

$$\left(\frac{\partial^2}{\partial x^2} + \frac{\partial^2}{\partial z^2}\right)\left(p - 0.5\mu_0\overline{\mu}M^2\right) = \frac{12\mu\dot{h}_0}{h^3}, \tag{9}$$

where μ is fluid viscosity, $\overline{\mu}$ is the magnetic susceptibility, and μ_0 stands for permeability of the free space.

It is easily observed that α, σ, and ε are all independent of x and while α and ε can assume both positive and negative values, σ is always positive. Following the averaging process discussed by Andharia et al. [24] and using (6), (9) takes the form

$$\left(\frac{\partial^2}{\partial x^2} + \frac{\partial^2}{\partial z^2}\right)\left(\overline{p} - 0.5\mu_0\overline{\mu}M^2\right) = \frac{12\mu\dot{h}_0}{m\left(\overline{h}\right)^{-1}}, \tag{10}$$

where $\overline{p}$ is the expected value of the lubricant pressure p while

$$\begin{aligned} m\left(\overline{h}\right) = \overline{h}^{-3}\Big[1 - 3\alpha\overline{h}^{-1} + 6\overline{h}^{-2}\left(\sigma^2 + \alpha^2\right) \\ -20\overline{h}^{-3}\left(\varepsilon + 3\sigma^2\alpha + \alpha^3\right)\Big]. \end{aligned} \tag{11}$$

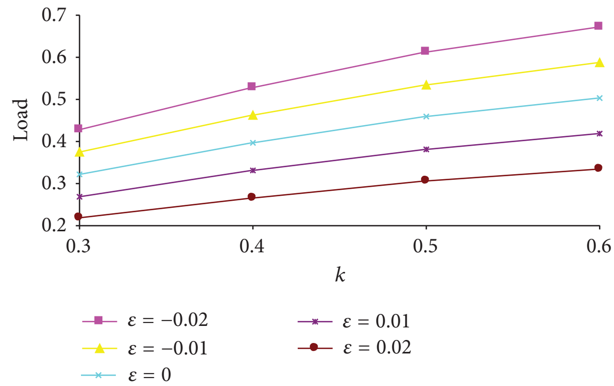

FIGURE 8: Variation of load carrying capacity with respect to k for different ε.

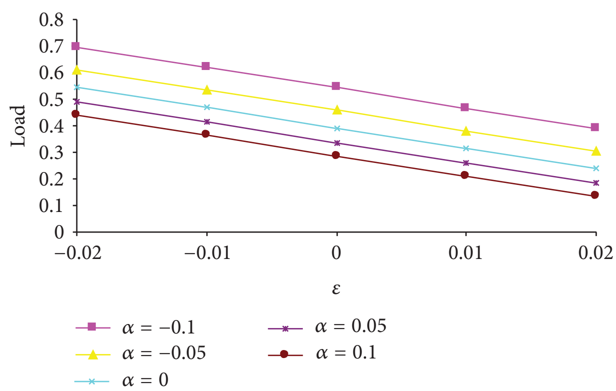

FIGURE 9: Variation of load carrying capacity with respect to ε for different α.

Introduction of dimensionless quantities:

$$H = \frac{\bar{h}}{h_0}, \quad X = \frac{x}{a}, \quad Z = \frac{z}{b},$$
$$M(H) = h_0^3 m(\bar{h}), \quad \bar{\alpha} = \frac{\alpha}{h_0}, \quad \bar{\sigma} = \frac{\sigma}{h_0}, \quad \bar{\varepsilon} = \frac{\varepsilon}{h_0},$$
$$k = \frac{b}{a}, \quad \mu^* = \frac{-\mu_0 \bar{\mu} h_0^3}{\mu \dot{h}_0}, \quad P = \frac{-\bar{p} h_0^3}{\mu \dot{h}_0 \pi a b}, \tag{12}$$

presents (10) in the form

$$\left(\frac{\partial^2}{\partial X^2} + \frac{\partial^2}{k^2 \partial Z^2}\right)\left(P - \frac{0.5\mu^* M^2}{\pi a b}\right) = \frac{12 M(H)}{k\pi}. \tag{13}$$

The associated boundary conditions are

$$P(X_1, Z_1) = 0; \quad X_1^2 + Z_1^2 = 1. \tag{14}$$

Solving (13) using boundary condition given in (14), one obtains the dimensionless pressure distribution:

$$P = \left[\frac{\mu^*}{2\pi}\left(1 + \frac{1}{k^2}\right) + \frac{6M(H)}{k\pi\left(1 + 1/k^2\right)}\right]\left(1 - X^2 - Z^2\right), \tag{15}$$

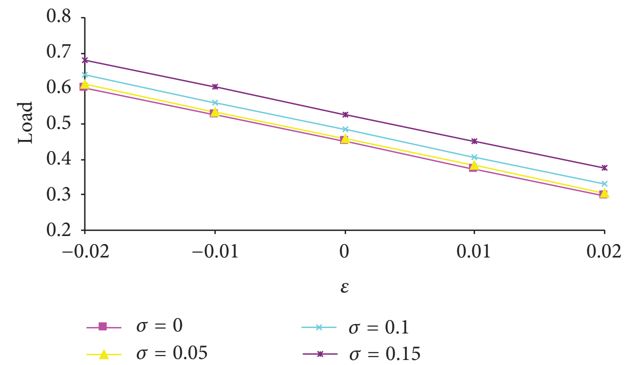

FIGURE 10: Variation of load carrying capacity with respect to ε for different σ.

where

$$M(H) = H^{-3}\left\lfloor 1 - 3\bar{\alpha}H^{-1} + 6H^{-2}\left(\bar{\sigma}^2 + \bar{\alpha}^2\right) - 20H^{-3}\left(\bar{\varepsilon} + 3\bar{\sigma}^2\bar{\alpha} + \bar{\alpha}^3\right)\right\rfloor. \tag{16}$$

The load carrying capacity of the bearing in non-dimensional form can be expressed as

$$W = \frac{1}{\pi}\int_{X=-1}^{X=1}\int_{Z=-\sqrt{1-X^2}}^{Z=\sqrt{1-X^2}} P\, dX\, dZ = \frac{\mu^*}{4\pi}\left(1 + \frac{1}{k^2}\right) + \frac{3M(H)}{k\pi\left(1 + 1/k^2\right)}. \tag{17}$$

3. Results and Discussion

It is easily observed that the non-dimensional pressure is determined from (15) while (17) presents the distribution of load carrying capacity in dimensionless form. It is clearly seen from these two equations that the dimensionless pressure increased by $(\mu^*/2\pi)(1 + 1/k^2)$ while load carrying capacity is increased by $(\mu^*/4\pi)(1 + 1/k^2)$ due to magnetic fluid lubricant. In the absence of roughness this study reduces to the performance of a magnetic fluid based squeeze film in elliptical plates.

To analyze the quantitative effect of various parameters such as the magnetization parameter μ^*, the aspect ratio $k(= b/a)$ and roughness parameters α, σ, and ε on the performance of the bearing, dimensionless load carrying capacity is computed numerically for different values of these parameters. Results are presented graphically in Figures 2, 3, 4, 5, 6, 7, 8, 9, 10, 11, 12, 13, 14, and 15.

In Figures 2, 3, 4, and 5 one can have the variation of load carrying capacity with respect to magnetization parameter for different values of α, σ, ε, and k, respectively. All these figures suggest that the load carrying capacity increases sharply with respect to the magnetization parameter. Figures 6, 7 and 8 depict the variation of load carrying capacity with respect to the aspect ratio k for different values of α, σ, and ε, respectively. From these figures one can easily observe that the increasing values of the aspect ratio cause increased load

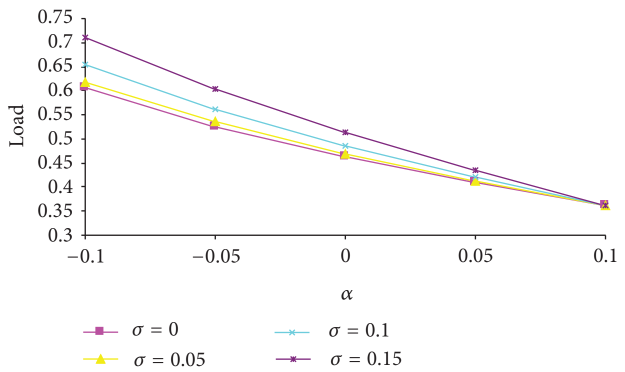

FIGURE 11: Variation of load carrying capacity with respect to α for different σ.

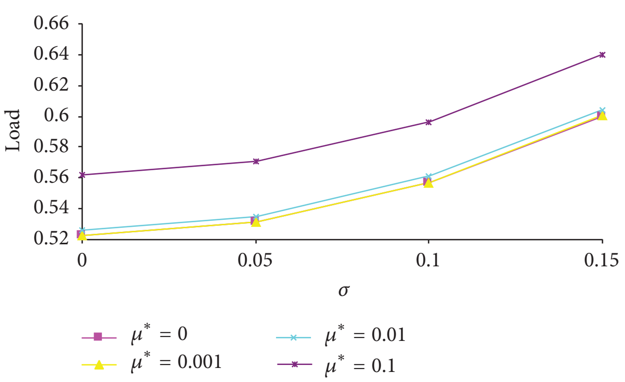

FIGURE 12: Variation of load carrying capacity with respect to σ for different μ^*.

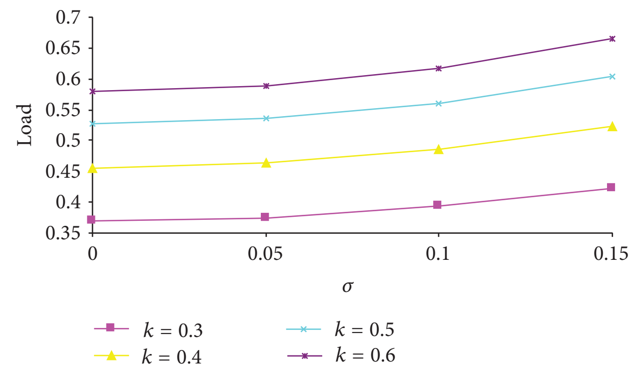

FIGURE 13: Variation of load carrying capacity with respect to σ for different k.

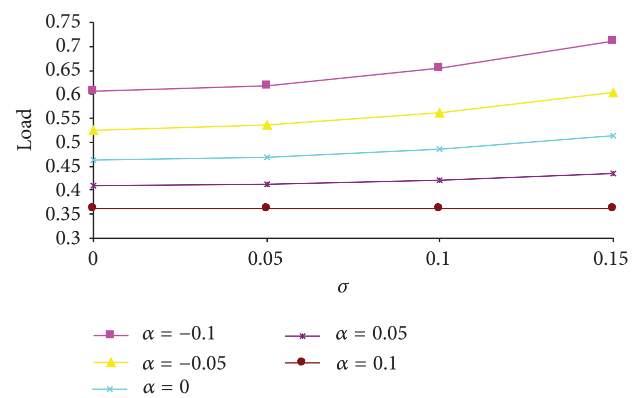

FIGURE 14: Variation of load carrying capacity with respect to σ for different α.

carrying capacity. Figures 9 and 10 give the profile for load carrying capacity with respect to the skewness for different values of α and σ respectively. It is clearly seen from these graphs that the positively skewed roughness decreases the load carrying capacity while the negatively skewed roughness increases the load carrying capacity. From Figure 11 it is observed that the trend of variance is quite similar to that of skewness so far as the distribution of load carrying capacity is concerned. It is also interesting to note that the effect of standard deviation is negligible beyond the variance's value 0.1 with regards to the distribution of load carrying capacity. Lastly, Figures 12, 13, 14, and 15 describe the variation of the load carrying capacity with respect to the standard deviation for various values of μ^*, k, α, and ε, respectively. Unlike the case of transverse roughness, here it is established that the standard deviation tends to increase the load carrying capacity. However, the increase at the initial stage is relatively less.

4. Conclusion

A close look at the figures reveals that the negative effect of positive α can be compensated to a considerable extent by the positive effect of the magnetization parameter by choosing a suitable aspect ratio in the case of negatively skewed roughness. In the similar way the negative effect of positive ε can be compensated by choosing suitable combination of magnetization parameter and aspect ratio especially when negative variance occurs.

Hence, this study makes it mandatory that the roughness must be given due consideration while designing the bearing system from bearing's life period point of view.

Nomenclature

a, b:	Dimensions of the bearing
h_0:	Film thickness
k:	Aspect ratio b/a
$\overline{M}$:	Magnetic field
M^2:	Magnitude of magnetic field
p:	Pressure in the film region
$\overline{p}$:	Expected value of the pressure
P:	Non-dimensional film pressure
w:	Load capacity
W:	Nondimensional load capacity
x, y, z:	Cartesian coordinates
α:	Mean of the stochastic film thickness
σ:	Standard deviation of the stochastic film thickness
ε:	Measure of symmetry of the stochastic film thickness

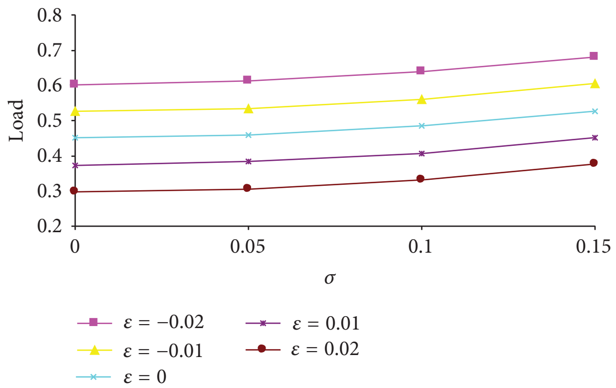

Figure 15: Variation of load carrying capacity with respect to σ for different ε.

σ^2: Variance
μ: Fluid viscosity
$\overline{\mu}$: Magnetic susceptibility
μ^*: Dimensionless magnetization parameter
μ_0: Permeability of the free space.

Acknowledgment

The authors are grateful to the referees for their valuable comments on the earlier version of the paper.

References

[1] F. R. Archibald, "Load capacity and time relations for squeeze films," *Transactions of the ASME*, vol. D78, pp. 231–245, 1956.

[2] H. Wu, "Squeeze film behaviour for porous annular disks," *Transactions of ASME*, vol. F92, pp. 593–596, 1970.

[3] H. Wu, "An analysis of the squeeze film between porous rectangular plates," *Transactions of ASME*, vol. F94, pp. 64–68, 1972.

[4] J. Prakash and S. Vij, "Load capacity and time-height relations for squeeze films between porous plates," *Wear*, vol. 24, no. 3, pp. 309–322, 1973.

[5] P. D. S. Verma, "Magnetic fluid based squeeze film," *International Journal of Engineering Science*, vol. 24, no. 3, pp. 395–401, 1986.

[6] M. V. Bhat and G. M. Deberi, "Squeeze film behaviour in porous annular discs lubricated with magnetic fluid," *Wear*, vol. 151, no. 1, pp. 123–128, 1991.

[7] M. V. Bhat and G. M. Deheri, "Magnetic fluid based squeeze film between two curved circular plates," *Bulletin of Calcutta Mathematical Society*, vol. 85, pp. 521–524, 1992.

[8] R. M. Patel and G. M. Deheri, "Magnetic fluid based squeeze film between porous conical plates," *Industrial Lubrication and Tribology*, vol. 59, no. 3, pp. 143–147, 2007.

[9] M. G. Davies, "The generation of pressure between rough fluid lubricated, moving, deformable surfaces," *Lubrication Engineering*, vol. 19, p. 246, 1963.

[10] R. A. Burton, "Effect of two dimensional sinusoidal roughness on the load support characteristics of a lubricant film," *Journal of Basic Engineering*, vol. 85, pp. 258–264, 1963.

[11] A. G. M. Michell, *Lubrication, Its Principle and Practice*, Blackie, London, UK, 1950.

[12] K. C. Tonder, "Surface distributed waviness and roughness," in *Proceedings of the 1st World Conference in Industrial Tribology*, vol. A3, pp. 1–8, New Delhi, India, 1972.

[13] S. T. Tzeng and E. Saibel, "Surface roughness effect on slider bearing lubrication," *Journal of Lubrication Technology*, vol. 10, pp. 334–338, 1967.

[14] H. Christensen and K. C. Tonder, *Tribology of Rough Surfaces: Stochastic Models of Hydrodynamic Lubrication*, SINTEF Report, no. 10/69–18, 1969.

[15] H. Christensen and K. C. Tonder, *Tribology of Rough Surfaces: Parametric Study and Comparison of Lubrication Models*, SINTEF Report, no. 22/69–18, 1969.

[16] H. Christensen and K. C. Tonder, "Hydrodynamic lubrication of rough bearing surfaces of finite width," *Journal of Lubrication Technology*, vol. 93, no. 3, 1971.

[17] L. L. Ting, "Engagement behaviour of lubricated porous annular disks part I: squeeze film phase, surface roughness and elastic deformation effects ," *Wear*, vol. 34, no. 2, pp. 159–182, 1975.

[18] J. Prakash and K. Tiwari, "Lubrication of a porous bearing with surface corrugations," *Journal of Lubrication Technology*, vol. 104, pp. 127–134, 1982.

[19] J. Prakash and K. Tiwari, "Roughness effects in porous circular squeeze—plates with arbitrary wall thickness," *Journal of Lubrication Technology*, vol. 105, no. 1, pp. 90–95, 1983.

[20] B. L. Prajapati, "Behaviour of squeeze film between rotating porous circular plates: surface roughness and elastic deformation effects," *Pure and Applied Mathematical Sciences*, vol. 33, no. 1/2, pp. 27–36, 1991.

[21] B. L. Prajapati, "Squeeze film behaviour between rotating porous circular plates with a concentric circular pocket: surface roughness and elastic deformation effects," *Wear*, vol. 152, no. 2, pp. 301–307, 1992.

[22] S. K. Guha, "Analysis of dynamic characteristics of hydrodynamic journal bearings with isotropic roughness effects," *Wear*, vol. 167, no. 2, pp. 173–179, 1993.

[23] J. L. Gupta and G. M. Deheri, "Effect of roughness on the behavior of squeeze film in a spherical bearing," *Tribology Transactions*, vol. 39, no. 1, pp. 99–102, 1996.

[24] P. I. Andharia, J. L. Gupta, and G. M. Deheri, "Effect of longitudinal surface roughness on hydrodynamic lubrication of slider bearings," in *Proceedings of the 10th International Conference on Surface Modification Technologies*, pp. 872–880, The Institute of Materials, 1997.

[25] P. I. Andharia and G. Deheri, "Longitudinal roughness effect on magnetic fluid-based squeeze film between conical plates," *Industrial Lubrication and Tribology*, vol. 62, no. 5, pp. 285–291, 2010.

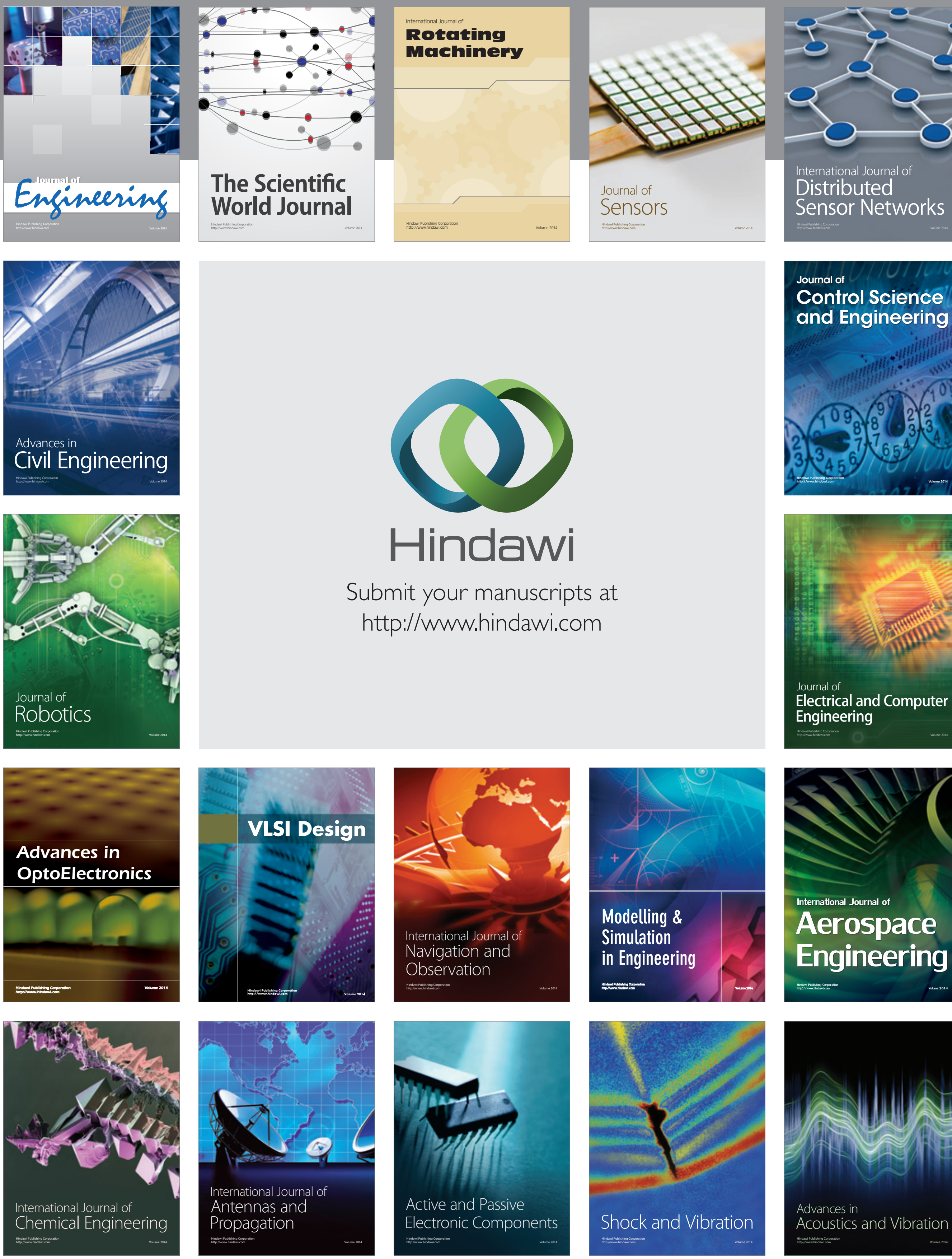
Journal of Engineering
The Scientific World Journal
International Journal of Rotating Machinery
Journal of Sensors
International Journal of Distributed Sensor Networks
Advances in Civil Engineering
Hindawi
Submit your manuscripts at
http://www.hindawi.com
Journal of Control Science and Engineering
Journal of Robotics
Journal of Electrical and Computer Engineering
Advances in OptoElectronics
VLSI Design
International Journal of Navigation and Observation
Modelling & Simulation in Engineering
International Journal of Aerospace Engineering
International Journal of Chemical Engineering
International Journal of Antennas and Propagation
Active and Passive Electronic Components
Shock and Vibration
Advances in Acoustics and Vibration